pH and salt effects on the aggregation behaviour of star polymer with G1 polyamidoamine core and terminal amphiphilic blocks

Hui Yang[ab]; Changchao Hu[a]; Xu Wu[ab]; Huibo Chen[a]; Jinben Wang[a]

[a] Key Laboratory of Colloid, Interface and Chemical Thermodynamics, Institute of Chemistry, The Chinese Academy of Sciences, Beijing, P.R. China [b] College of Materials Science and Chemical Engineering, Harbin Engineering University, Harbin, P.R. China

PLEASE SCROLL DOWN FOR ARTICLE

pH and salt effects on the aggregation behaviour of star polymer with G1 polyamidoamine core and terminal amphiphilic blocks

Hui Yang[ab], Changchao Hu[a], Xu Wu[ab], Huibo Chen[a] and Jinben Wang[a]*

[a]*Key Laboratory of Colloid, Interface and Chemical Thermodynamics, Institute of Chemistry, The Chinese Academy of Sciences, Beijing 100190, P.R. China;* [b]*College of Materials Science and Chemical Engineering, Harbin Engineering University, Harbin 150001, P.R. China*

In this study, the pH and salt effects on the aggregation behaviour of star polymer, with G1 polyamidoamine as the core and poly(propylene oxide)-*block*-poly(ethylene oxide) as the terminal branches, were investigated. The results from pH and turbidimetric titration experiments showed that with the pH value increasing from 2.0 to 10.0, the solution transforms from transparent to turbid at $pK_a = 5.5$ and eventually presents phase separation at the pH value above 7.5. As revealed by dynamic light scattering and transmission electron microscopy measurements, the size of the aggregates of star polymer becomes bigger with the increase in the pH value or in the presence of salt. It was found that the extent of the salt effect on the aggregation behaviour follows the sequence: $C_6H_5COONa > Na_2SO_4 > NaCl$.

Keywords: star polymer; supramolecule; aggregation behaviour; pH effect; salt effect

1. Introduction

Owning a highly symmetrical, branched, three-dimensional and supramolecular architecture, star polymers represent an intriguing approach to controlling molecular organisation at the colloidal scale in contrast to conventional colloids (*1, 2*). Since the pioneer work and development of related cascade molecules appeared in the past two decades (*3–8*), radial structures have been designed and created extensively. To date, various examples of polyamidoamine (PAMAM)-based star polymers binding metal ions or functionalised with rigid hydrophobic periphery have been investigated intensively (*9–12*). Little attention, however, has been paid to the aggregation behaviour of PAMAM molecules branched with amphiphilic segments (*13*), though this kind of star polymers has great importance in many potential application fields (*14–16*).

The effects of additional salts on the aggregation behaviour of radial surfactants in aqueous solution are especially vital for detergency and emulsification in industry (*17*). Furthermore, the adjustment of the pH environment of some star polymer solutions can obviously affect its aggregation behaviour (*18*). Hence, it is very important to investigate the star polymers in aqueous environments with various acidity or ionic strengths for many applications (*17, 19*). We have reported the synthesis, surface and aggregation properties of a series of PAMAM-based star polymers branched with poly(propylene oxide) (PPO)-*block*-poly(ethylene oxide) (PEO) (*20, 21*), and found that the aggregation property of the polymers is not only related to their molecular structure, but also to their sensitivity to the pH value and ionic strength. The present work, as a further research, mainly focuses on the pH and salt effects on the aggregation properties of the synthesised amphiphilic star polymer in aqueous solution. The aim is to examine the change in the aggregation of the polymer systems with the variation in the pH values or salt species.

2. Experimental section

2.1 Materials

Pyrene was purchased from Aldrich (Milwaukee, WI, USA) and recrystallised from ethanol before use. Ethylenediamine, propylene oxide (PO), ethylene oxide (EO), sodium benzoate and other chemicals were obtained from Beijing Chemical Reagents Company (Beijing, China) and were of analytical grade.

2.2 Synthesis and characterisation

The synthesis and characterisation of the PAMAM-based star polymer were carried out as described in our earlier work (*20, 21*). The key characteristic parameters of the polymer are presented in Table 1.

*Corresponding author. Email: jbwang@iccas.ac.cn

Table 1. Characteristic parameters of the PAMAM-based radial molecule.

	Polydispersity, M_w/M_n	Weight average, M_w	Core content, G1-PAMAM (wt%)	PO:EO (mass ratio)	PPO$_x$-b-PEO$_y$ (x, y = group number per chain)	
					x	y
Characteristic parameters	1.30	51,600	1	3:1	55	24

2.3 Measurements

2.3.1 Turbidimetric titration

The turbidity of the star polymer solution with different salts and pH values was measured at 450 nm using a Brinkman PC920 probe colorimeter equipped with a thermostated water-circulating bath. The cloud point (CP) of the polymer at different conditions was obtained from the break of the $100 - T\%$ (transmittance) vs. the temperature curves.

2.3.2 pH titration

The pH value of the solution with the star polymer concentration of 1 wt% was adjusted to 2.0, and then it was titrated using dilute NaOH solution, monitored with a pHS-2C acidity meter at a temperature of $25.0 \pm 0.1^\circ$C. The titration was repeated thrice, and the average of the pK_a values was calculated.

2.3.3 Steady-state fluorescence measurements

Pyrene was employed as the probe with the concentration of around 1 μM. It was excited at 335 nm, and the emission spectrum was scanned from 350 to 550 nm. I_1/I_3 is the ratio of the fluorescence intensities of the pyrene emission spectrum at 373 nm (I) and 384 nm (III), which was used to evaluate the variation in the micropolarity of the star polymer aggregates. Tests were carried out on a Hitachi F-4500 fluorescence spectrophotometer at $25.0 \pm 0.5^\circ$C.

2.3.4 Dynamic light scattering

Dynamic light scattering (DLS) measurement was carried out using an LLS spectrometer (ALV/SP-125) with a multi-τ digital time correlator (ALV-5000). Light ($\lambda = 632.8$ nm) from a solid-state He–Ne laser (22 mW) was used as the incident beam. The scattering angle was selected as 90° and the correlation function was analysed with the CONTIN method. The solutions were filtrated through 0.45 μm millipore to leach the dust before measurements.

2.3.5 Transmission electron microscope

Sample imaging was carried out using transmission electron microscope (TEM) in the systems of a Hitachi H800 microscope. Negative-staining (with uranyl acetate aqueous solution of 1 wt%) and freeze-fracture (FF) techniques were used for TEM sample preparation. Fracturing and replication were carried out in a high-vacuum freeze-etching system (Balzers BAF-400D). TECNAI-20 electron microscope was employed for the microscopic observation.
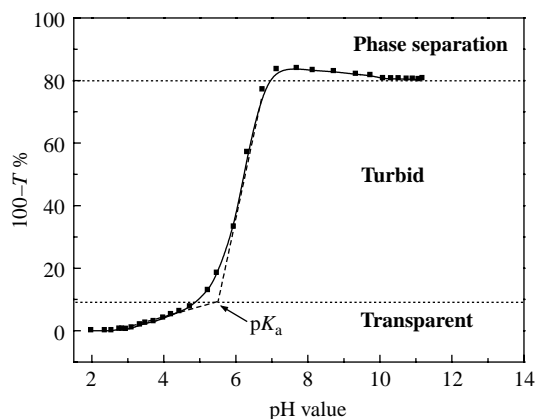

Figure 1. Variation of turbidity with pH values at $25.0 \pm 0.1^\circ$C.
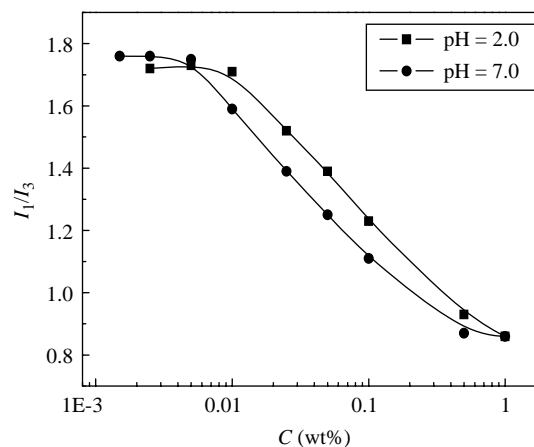

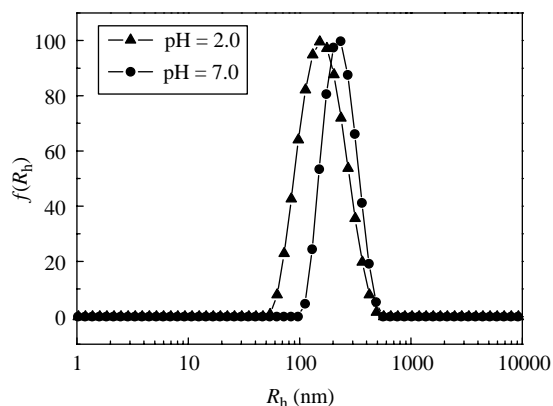Figure 2. Variation of I_1/I_3 with the star polymer concentration at different pH values.

Figure 3. Size distribution of the star polymer aggregates at different pH values and $25.0 \pm 0.1^{\circ}$C.

3. Results and discussion

A non-ionic surfactant solution above its critical micelle concentration (CMC) turns turbid after being heated to a certain temperature, known as the CP temperature (*22*). Usually, at CP, both the size and the number of aggregates are vital for visible turbidity (*23*). In Figure 1, a sigmoid

curve can be observed and the value of $pK_a = 5.5$ can be obtained from the point of break. When the pH is below pK_a, the solution is transparent, mainly due to the complete protonation of the amide group of PAMAM; in the case of pK_a ($= 5.5$) $<$ pH $<$ 7.5, the solution becomes turbid, because the protonation process becomes incomplete, which may also lead the star polymer molecules to form bigger aggregates. However, when pH $>$ 7.5, protonation cannot be carried out, leading to phase separation.

Steady-state fluorescence measurement was performed to examine the polarity of the microenvironment of the star polymer aggregates, as indicated by the change in the intensity ratio I_1/I_3 of pyrene, under the variation in the pH value. Figure 2 shows that, at a higher pH value, an earlier break at the critical aggregation concentration (CAC) occurs and the polarity is lower at the concentration range above the CAC, mainly because of the incomplete protonation process of the amide groups under neutral environment, which supports the result obtained from turbidimetric measurement.

DLS and TEM measurements were carried out to examine the size distribution and morphology of the aggregates, and the results are shown in Figures 3 and 4,
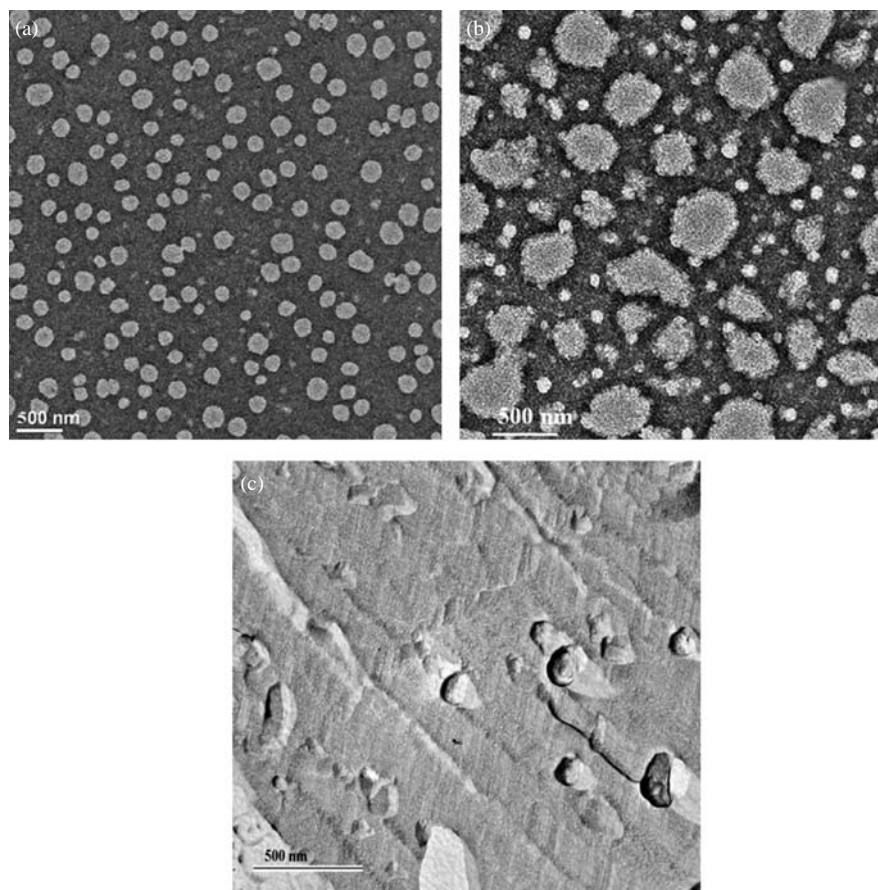

Figure 4. TEM images of the star polymer aggregates at: (a) pH 2.0 (negative-staining); (b) pH 7.0 (negative-staining) and (c) pH 2.0 (FF).
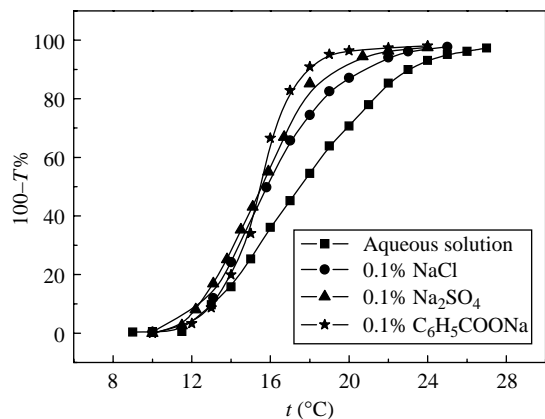
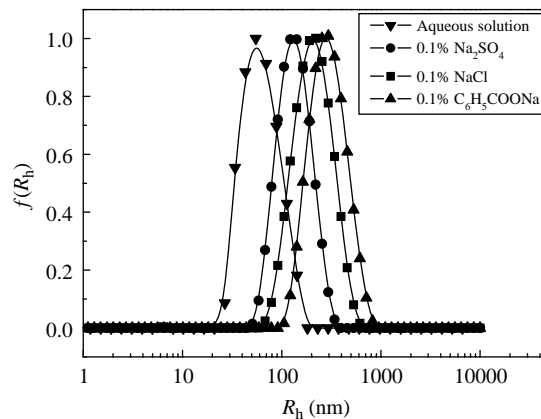Figure 5. Variation of turbidity with temperature in the presence of different salts.

Figure 6. DLS measurements of the size distribution for the star polymer aggregates in the presence of different salts at $15.0 \pm 0.1^{\circ}C$.

respectively. From Figure 3, it can be observed that the mean hydrodynamic radius (R_h) is about 151 nm at pH 2.0 and 233 nm at pH 7.0. The size increase with the pH value is mainly attributed to the extent of protonation, being in favour of the variation tendency of the size of the aggregates indicated from pH titration measurement.

Negative-staining TEM observation results are shown in Figure 4(a) and (b) in which spherical aggregates can be observed. The size of the aggregates is in the range of 200–300 nm at pH 2.0 and 400–500 nm at pH 7.0. Figure 4(c) shows the FF-TEM image and reveals an average size of around 200 nm at pH 2.0, matching with the negative-staining TEM result (Figure 4(a)). All the TEM experimental results are in good agreement with those from the DLS measurement.

The turbidity curves of 1% star polymer with and without added salt are exhibited in Figure 5. The CP values obtained are listed in Table 2, from which it can be seen that the CP value increases with different salts in the order: $NaCl > Na_2SO_4 > C_6H_5COONa$. In other words, the salt effect on the aggregation behaviour is in the decreasing order: $C_6H_5COONa > Na_2SO_4 > NaCl$. The effect of SO_4^{2+} and Cl^- is mainly attributed to the hydration interaction (24, 25), namely the more preferential movement of water molecules from coordination shells of star polymer molecules to the hydration shells of SO_4^{2+} than that of Cl^-. The salt effect of C_6H_5COONa mostly lies on

the role of the benzene ring which may penetrate into the hydrophobic core of the aggregates (26) and, therefore, this kind of organic salt has a great effect on the growth of the aggregate sizes.

Figure 6 shows the size distribution of the star polymer aggregates with and without the influence of salt. The R_h values are listed in Table 2, from which we can observe that the salts have an effect on the aggregation behaviour, resulting in the growth of the aggregates.

A collection of spherical aggregates with the size of around 300, 400 and 600 nm is observed as exhibited in Figure 7(a) (negative-staining) and (d) (FF), (b) (negative-staining) and (c) (negative-staining), respectively, which is in agreement with the aggregate size obtained from the DLS results.

4. Conclusion

In this study, the pH and salt effects on the aggregation behaviour of PAMAM-based star polymer in aqueous solution were investigated. When the acidity is below 5.5 (pK_a value), the polymer solution is transparent mostly because of the thorough protonation of the amide group of PAMAM; when the pH is in the range of 5.5–7.5, the protonation process becomes incomplete, which leads the star polymer molecules to form bigger aggregates. However, when the environment is basic, protonation cannot take place and the oil phase separates out. With the increasing pH value, the CAC value becomes lower and the microenvironment becomes less polar at the concentration above the CAC, mainly due to the incomplete protonation process under the neutral environment. The salt effect on the aggregation behaviour is in the decreasing order: $C_6H_5COONa > Na_2SO_4 > NaCl$, resulting in the increase in CP temperature. The effect of inorganic salts is mainly attributed to the hydration process

Table 2. CP temperature and hydrodynamic radius (R_h) of the aggregates in the presence of different salts.

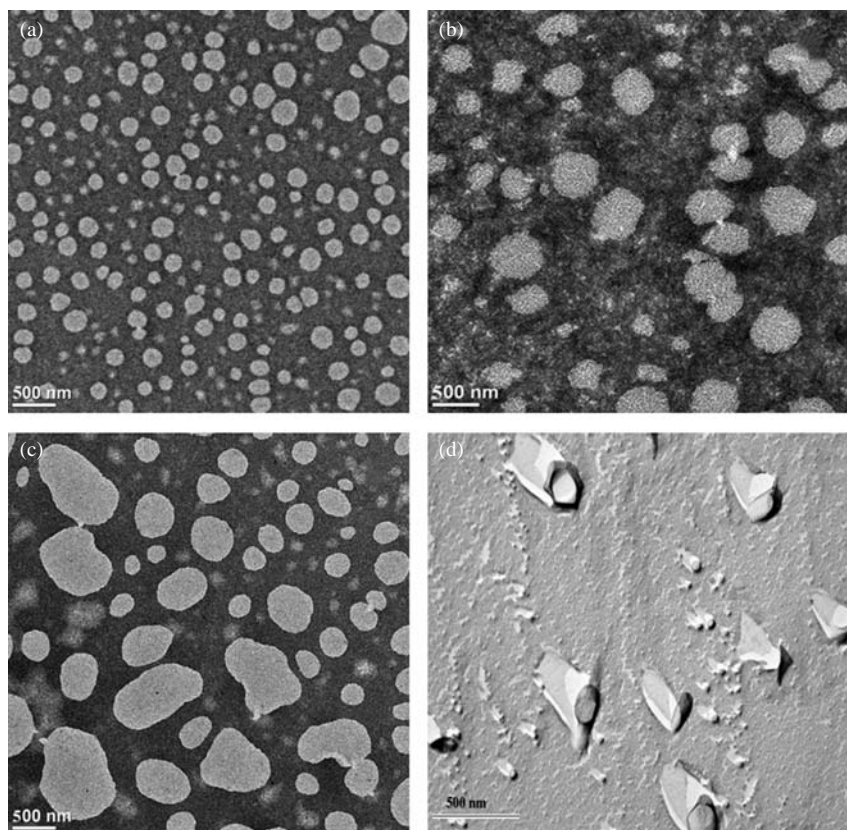|	1% PAMAM-based star polymer			
		in salt aqueous solution (0.1 wt% salt)		
	in water	Na_2SO_4	NaCl	C_6H_5COONa
CP (°C)	22.5	18.5	20.2	17.3
R_h (nm)	55	140	223	300

Figure 7. TEM images of the star polymer aggregates in the presence of different salts: (a) 0.1 wt% Na_2SO_4 (negative-staining); (b) 0.1 wt% NaCl (negative-staining); (c) 0.1 wt% C_6H_5COONa (negative-staining) and (d) 0.1 wt% Na_2SO_4 (FF).

of the preferential movement of water molecules from the coordination shells of the star polymer molecules to the hydration layer of the salt molecules, and the benzene ring of the organic salt affects the aggregation behaviour to a great extent, owing to the penetration into the hydrophobic core of the aggregates.

Acknowledgements

References

(1) Meltzer, A.D.; Tirrell, D.A.; Jones, A.A.; Inglefield, P.T.; Hedstrand, D.M.; Tomalia, D.A. *Macromolecules* **1992**, *25*, 4541–4548.

(2) Bosman, A.W.; Janssen, H.M.; Meijer, E.W. *Chem. Rev.* **1999**, *99*, 1665–1688.

(3) Buhleier, E.; Wehner, W.; Vögtle, F. *Synthesis* **1978**, *2*, 155–158.

(4) Maciejewski, M. *J. Macromol. Sci.* **1982**, *A17*, 689–703.

(5) Newkome, G.R.; Yao, Z.; Baker, G.R.; Gupta, V.K. *J. Org. Chem.* **1985**, *50*, 2003–2004.

(6) Tomalia, D.A.; Baker, H.; Dewald, J.; Hall, M.; Kallos, G.; Martin, S.; Roeck, J.; Ryder, J.; Smith, P. *Macromolecules* **1986**, *19*, 2466–2468.

(7) Hawker, C.J.; Fréchet, J.M.J. *J. Am. Chem. Soc.* **1990**, *112*, 7638–7647.

(8) Miller, T.M.; Neenan, T.X. *Chem. Mater.* **1990**, *2*, 346–349.

(9) Yang, L.; Luo, Y.; Jia, X.; Ji, Y.; You, L.; Zhou, Q. *J. Phys. Chem. B* **2004**, *108*, 1176–1178.

(10) Jiang, D.L.; Aida, T. *J. Am. Chem. Soc.* **1998**, *120*, 10895–10901.

(11) Yeow, E.K.; Ghiggino, K.P.; Reek, J.N.; Crossley, M.J.; Bosman, A.W.; Schenning, A.P.; Meijer, E.W. *J. Phys. Chem. B* **2000**, *104*, 2596–2606.

(12) Diallo, M.S.; Arasho, W.; Johnson, J.H., Jr., Goddard, W.A., III. *Environ. Sci. Technol.* **2008**, *42*, 1572–1579.

(13) Xin, X.; Xu, G.Y.; Zhang, Z.Q.; Chen, Y.J.; Wang, F. *Eur. Polym. J.* **2007**, *43*, 3106–3111.

(14) King, A.S.H.; Martin, I.K.; Twyman, L.J. *Polym. Int.* **2006**, *55*, 798–807.

(15) Wang, J.; Li, C.Q.; Li, J.; Yang, J.Z. *Sep. Sci. Technol.* **2007**, *42*, 2111–2120.

(16) Escudero, A.G.; Azagarsamy, M.A.; Theddu, N.; Vachet, R.W.; Thayumanavan, S. *J. Am. Chem. Soc.* **2008**, *130*, 11156–11163.

(17) Porcar, L.; Liu, Y.; Verduzco, R.; Hong, K.L.; Butler, P.D.; Magid, L.J.; Smith, G.S.; Chen, W.R. *J. Phys. Chem. B* **2008**, *112*, 14772–14778.

(18) Diallo, M.S.; Falconer, K.; Johnson, J.H.; Goddard, W.A. *Environ. Sci. Technol.* **2007**, *41*, 6521–6527.

(19) Meijer, E.W.; van Genderen, M.H.P. *Nature (London)* **2003**, *426*, 128–129.

(20) Zhang, W.; Dong, G.; Yang, H.; Sun, J.; Zhou, J.; Wang, J. *Colloid Surf. A* **2009**, *348*, 45–48.

(21) Yang, H.; Han, Y.; Yang, S.; Zhang, W.; Tan, G.; Wang, Y.; Wang, J. *Supramol. Chem.* **2009**, *21*, 754–758.

(22) D'Errico, G.; Paduano, L.; Khan, A. *J. Colloid Interface Sci.* **2004**, *279*, 379–390.

(23) Zhao, G.Q.; Chen, S.B. *Langmuir* **2006**, *22*, 9129–9134.

(24) Grover, P.K.; Ryall, R.L. *Chem. Rev.* **2005**, *105*, 1–10.

(25) Eucken, A.; Hertzberg, G.Z. *Phys. Chem.* **1950**, *195*, 1–23.

(26) Lu, T.; Huang, J.; Li, Z.; Jia, S.; Fu, H. *J. Phys. Chem. B* **2008**, *112*, 2909–2914.